HUMAN GENE THERAPY METHODS 24:28–37 (February 2013)

DOI: 10.1089/hgtb.2012.197

Induction of Aberrant Vascular Growth, But Not of Normal Angiogenesis, by Cell-Based Expression of Different Doses of Human and Mouse VEGF Is Species-Dependent

Edin Mujagic,[1,2*] Roberto Gianni-Barrera,[1*] Marianna Trani,[1*] Abdulsamie Patel,[1] Lorenz Gürke,[2] Michael Heberer,[1] Thomas Wolff,[1,2] and Andrea Banfi[1]

Abstract

Therapeutic angiogenesis by vascular endothelial growth factor (VEGF) gene delivery is an attractive approach to treat ischemia. VEGF remains localized around each producing cell *in vivo*, and overexpression of mouse $VEGF_{164}$ ($mVEGF_{164}$) induces normal or aberrant angiogenesis, depending strictly on its dose in the microenvironment *in vivo*. However, the dose-dependent effects of the clinically relevant factor, human $VEGF_{165}$ ($hVEGF_{165}$), are unknown. Here we exploited a highly controlled gene delivery platform, based on clonal populations of transduced myoblasts overexpressing specific VEGF levels, to rigorously compare the *in vivo* dose-dependent effects of $hVEGF_{165}$ and $mVEGF_{164}$ in skeletal muscle of severe combined immune deficient (SCID) mice. While low levels of both factors efficiently induced similar amounts of normal angiogenesis, only high levels of $mVEGF_{164}$ caused widespread angioma-like structures, whereas equivalent or even higher levels of $hVEGF_{165}$ induced exclusively normal and mature capillaries. Expression levels were confirmed both *in vitro* and *in vivo* by enzyme-linked immunosorbent assay (ELISA) and quantitative reverse-transcriptase polymerase chain reaction (qRT-PCR). However, *in vitro* experiments showed that $hVEGF_{165}$ was significantly more effective in activating VEGF receptor signaling in human endothelial cells than $mVEGF_{164}$, while the opposite was true in murine endothelial cells. In conclusion, we found that, even though hVEGF is similarly efficient to the syngenic mVEGF in inducing angiogenesis at lower doses in a widely adopted and convenient mouse preclinical model, species-dependent differences in the relative activation of the respective receptors may specifically mask the toxic effects of high doses of the human factor.

Introduction

Coronary artery disease and peripheral vascular disease are a major cause of morbidity and mortality in Western societies despite current medical and surgical treatment (Norgren *et al.*, 2007). Therapeutic angiogenesis aims at inducing new blood vessels by the delivery of vascular growth factors in order to increase the perfusion of tissue distal to a vascular occlusion, and it is a promising strategy for the treatment of many patients for whom there is currently no effective surgical or medical treatment. Vascular endothelial growth factor-A (VEGF) is the master regulator of angiogenesis (Carmeliet, 2003). VEGF gene therapy with different vectors has been investigated in several clinical trials for both peripheral and coronary artery disease. However, despite initial positive results, placebo-controlled phase II studies have not shown clear clinical efficacy (Gupta *et al.,* 2009). Retrospective analyses found that a crucial problem is the difficulty to achieve sufficient angiogenesis in the target tissue at safe vector doses (Yla-Herttuala *et al.*, 2004; Gupta *et al.,* 2009; Karvinen and Yla-Herttuala, 2010), highlighting the need to carefully determine the therapeutic window of VEGF dose *in vivo* in order to increase efficacy of the treatments.

Human VEGF has been shown to effectively induce angiogenesis in many other species, including rodents, rabbits, and pigs, thereby allowing clinically relevant questions to be investigated in convenient animal models. In particular, information about the dose-dependent toxic effects is fundamental to guide the design of clinical trials. It has been shown that the uncontrolled expression of murine VEGF in

[1]Cell and Gene Therapy, Department of Biomedicine and Department of Surgery, Basel University Hospital and Basel University, Basel CH-4031, Switzerland.
[2]Vascular Surgery, Department of Surgery, Basel University Hospital, Basel CH-4031, Switzerland.
*These authors contributed equally to this work.

rodent preclinical models by a variety of methods leads to progressive vascular proliferation and eventually the growth of angioma-like vascular tumors (Springer *et al.*, 1998; Carmeliet, 2000; Lee *et al.*, 2000; Pettersson *et al.*, 2000). However, reports of similar consequences by the delivery of human VEGF in rodent models have been very rare (Schwarz *et al.*, 2000), prompting the question of whether the human and murine factors may have intrinsically different effects or whether mouse models may not be reliable to determine the dose-dependent toxicity of human VEGF.

The VEGF molecule exists as at least three major isoforms of 120/121, 164/165, and 188/189 amino acids in mouse and in man, respectively, which differ in the size of their heparin-binding domain and therefore in their avidity for extracellular matrix (Park *et al.*, 1993). Elegant studies with transgenic mice selectively expressing only one of the three isoforms showed that, while $VEGF_{120}$ and $VEGF_{188}$ alone caused defective vascular morphogenesis, with respectively excessive vessel size and insufficient branching, or the reverse, $VEGF_{164}$ could induce physiological vascular networks even in the absence of the other isoforms (Ruhrberg *et al.*, 2002), making $VEGF_{164/165}$ the preferred choice for therapeutic over-expression.

$VEGF_{164/165}$ remains tightly localized in the extracellular matrix (Park *et al.*, 1993; Springer *et al.*, 2003). Therefore, heterogeneous levels in tissue do not average with each other, and we have previously found that the induction of normal or aberrant angiogenesis by mouse $VEGF_{164}$ depends strictly on the amount produced in the microenvironment around each producing cell and not on the total dose (Ozawa *et al.*, 2004; von Degenfeld *et al.*, 2006). The delivery of different titers of gene therapy vectors only influences the total dose but cannot uncover the effects of specific microenvironmental expression levels. Therefore, in this study we took advantage of a highly controlled platform for VEGF expression in mouse muscle (Ozawa *et al.*, 2004; von Degenfeld *et al.*, 2006), based on clonal populations of transduced myoblasts homogeneously producing specific factor levels to rigorously compare the *in vivo* dose-dependent effects of human and mouse $VEGF_{164/165}$.

Materials and Methods

Vector construction

A bicistronic construct, carrying a truncated version of the mouse CD8a gene the mouse $VEGF_{164}$ gene linked to, was generated. For mouse CD8 the truncated version Lyt-2, or Lyt-2.2 (trCD8a), occurs naturally by alternative splicing, spanning codons 1–222, and it includes the signal peptide, the full extracellular, and transmembrane regions, whereas the cytoplasmic region is truncated after the first two amino acids (221–222) (Tagawa *et al.*, 1986). The full retroviral construct (mV) was generated by cloning the cDNAs encoding mouse $VEGF_{164}$ and mouse trCD8a upstream and downstream of an encephalomyocarditis virus internal ribosomal entry sequence (IRES). The control construct (mCD8) contained the IRES and mouse trCD8a sequences but no sequence for VEGF.

Correspondingly, a similarly truncated version of the human CD8 gene was generated by PCR from the full-length transcript (a kind gift by Dan Littman), and the corresponding constructs containing the genes for human $VEGF_{165}$, IRES, and trCD8a (hV), and the control construct containing IRES and human trCD8a but no VEGF (hCD8) were cloned.

Cell culture

Primary myoblasts, isolated from C57BL/6 mice and already transduced to express the β-galactosidase marker gene (lacZ) from a retroviral promoter (Rando and Blau, 1994), were further transduced at high efficiency with the retroviral constructs described above for four rounds of infection, as previously described (Springer and Blau, 1997). Early passage myoblast clones homogeneously expressing specific levels of VEGF were isolated by randomly sorting single cells in 96-wells, using a FACS Vantage SE cell sorter (Becton Dickinson, Basel, Switzerland). Cells were cultured in 5% CO_2 on dishes coated with bovine skin collagen 1 (Sigma-Aldrich Chemie GmbH, Steinheim, Germany), with a growth medium consisting of 40% F10, 40% low-glucose Dulbecco's modified Eagle's medium (DMEM; Sigma-Aldrich), and 20% fetal bovine serum (HyClone, Logan, UT) supplemented with 2.5 ng/ml of basic fibroblast growth factor (FGF-2; Becton Dickinson), as previously described (Banfi *et al.*, 2002).

CD8 detection by FACS

Expression of human trCD8a and mouse trCD8a was assessed by staining-transduced myoblasts with specific APC-conjugated antibodies under experimentally determined optimal conditions, as previously described (Misteli *et al.*, 2010). The mouse anti-human CD8 (clone 3B5; Caltag Laboratories Inc, Burlingame) was used at 0.5 μg of antibody/10^6 cells, at a dilution of 1:50. The rat anti-mouse CD8 (clone 53-6.7; Becton Dickinson) was used at 0.8 μg of antibody/10^6 cells, at a dilution of 1:50. Data were acquired with a FACSCalibur flow cytometer (Becton Dickinson) and analyzed using FlowJo software (Tree Star, Ashland, Oregon).

Human and mouse VEGF quantification by ELISA

The production of VEGF in cell culture supernatants was quantified using species-specific VEGF immunoassay ELISA kits (R&D Systems Europe, Abingdon, United Kingdom) according to manufacturer's instructions. One ml of fresh medium was incubated on myoblasts cultured in a 60-mm dish for 4 hr, then filtered and analyzed in duplicate. Results were normalized by the number of cells and expressed as ng of VEGF per 10^6 cells per day. At least four separate dishes of cells were assayed for each clone.

Myoblast injection into severe combined immune deficient mice

For the evaluation of angiogenesis *in vivo*, cells were implanted into 6–8-week-old severe combined immune deficient (SCID) CB.17 mice (Charles River Laboratories, Sulzfeld, Germany) in order to avoid an immunological response to myoblasts expressing xenogenic proteins. Animals were treated in accordance with Swiss Federal guidelines for animal welfare, and the study protocol was approved by the Veterinary Office of the Canton of Basel-Stadt (Basel, Switzerland). Myoblasts were dissociated in trypsin and resuspended in phosphate-buffered saline (PBS) with 0.5% BSA; 5×10^5 myoblasts in 5 μl were implanted by intramuscular injections into the posterior auricular muscle, midway up the dorsal aspect of the external ear or into the tibialis anterior muscle of the hind limb, using a syringe with a $29^1/_2$G needle.

Tissue staining

In order to visualize the entire vascular network of the ear, we performed intravascular staining with a biotinylated *Lycopersicon esculentum* (tomato) lectin (Vector Laboratories, Burlingame, California), which binds the luminal surface of all blood vessels, as previously described (Ozawa *et al.*, 2004). Briefly, 4 weeks after myoblast implantation, mice were anesthetized and lectin was injected intravenously through the femoral vein. Four minutes later the thoracic cavity was opened and the tissues were fixed by perfusing the animal with 1% paraformaldehyde and 0.5% glutaraldehyde in PBS, pH 7.4 at 120 mmHg of pressure via a cannula in the left ventricle. Ears were then removed, bisected in the plane of the cartilage, and stained with X-gal staining buffer (1 mg/ml 5-bromo-4-chloro-3-indoyl-b-D-galactoside, 5 m*M* potassium ferrocyanide, 0.02% Nonidet P-40, 0.01% sodium deoxycholate, 1 m*M* $MgCl_2$, in PBS, pH 7.4). Lectin-coated vessels were stained using avidin-biotin complex-diaminobenzidine histochemistry (Vector Laboratories), dehydrated through an ethanol series from 50% to 98%, cleared with toluene (Fisher Scientific, Wohlen, Switzerland) and whole-mounted on glass slides with Permount embedding medium (Fisher Scientific, Wohlen, Switzerland). To obtain limb muscle sections, animals were anesthetized and tissues were fixed by perfusion of 1% paraformaldehyde in PBS, pH 7.4 at 120 mmHg of pressure via a cannula in the left ventricle. The tibialis anterior muscle was harvested in one piece, cryoprotected in 10% sucrose overnight, embedded in OCT compound (Sakura Finetek, Torrance, California), frozen in freezing isopentane and cryosectioned. Tissue sections were then stained with X-gal (20 μm sections) or with H&E (10 μm sections) as described previously (Rando and Blau, 1994). Further 10-μm sections were immunostained as described previously (Ozawa *et al.*, 2004). The following primary antibodies and dilutions were used: rat monoclonal anti-mouse CD31 (clone MEC 13.3; BD Biosciences) at 1:100; mouse monoclonal anti-mouse α-smooth muscle actin (α-SMA) (clone 1A4; MP Biomedicals, Irvine, CA) at 1:400; rabbit polyclonal anti-NG2 (Chemicon, Temecula, CA) at 1:200. Fluorescently labeled secondary antibodies (Invitrogen, Basel, Switzerland) were used at a concentration of 1:200.

Vessel measurements

Regions of myoblast engraftment were determined by identifying β-galactosidase-positive muscle fibers on whole-mounted ears. Images were taken on an Olympus BX61 microscope. Vessel length density (VLD) was measured as described previously (Ozawa *et al.*, 2004). Briefly, the total vessel length was manually traced on images taken in 3–6 fields of vision per ear, divided by the area of the field of vision and expressed in mm/mm^2. Image analysis was performed with the AnalySIS D software (Soft Imaging System Gmbh, Münster, Germany).

Isolation of proteins, genomic DNA and total RNA in muscle tissue

Whole fresh mouse muscles were disrupted using a Qiagen Tissue Lyser (Qiagen, Hilden, Germany) in 500 μl of PBS + 1% Triton X-100, supplemented with Complete Protease Inhibitor Cocktail (Roche), which was nondenaturing for proteins and did not lyse nuclei. After centrifugation, 200 μl aliquots of the lysates were used for protein quantification and ELISA analysis. The remaining supernatant (on average 250 μl) was used to extract total RNA with the all-Prep DNA/RNA/protein Mini kit (Qiagen), after supplementation with the denaturing buffer provided by the manufacturer. The pellet containing the whole nuclei was then disrupted and homogenized in the same lysis buffer using the Qiagen Tissue Lyser. Genomic DNA was extracted using the same kit following the manufacturer's instructions.

Quantitative real-time PCR

Total RNA was reverse-transcribed into cDNA with the Omniscript Reverse Transcription kit (Qiagen) at 37°C for 60 min. Quantitative real-time PCR (qRT-PCR) was performed on an ABI 7300 Real-Time PCR system (Applied Biosystems, Carlsbad, CA). In order to quantify both the human $VEGF_{165}$ and mouse $VEGF_{164}$ transcripts and to compare their expression, a unique set of primers and probe sequences was designed with Primer Express software 3.0 (Applied Biosystems), based on a common sequence expressed by both the human and mouse VEGF retroviral constructs: ExoV forward: 5′-GCTCTCCTCAAGCGTATTC AACA; ExoV reverse: 5′-CCCCAGATCAGATCCCATACA; ExoV probe: 5′-FAM-CTGAAGGATGCCCAGAAGGTA CCCCA-TAMRA. Furthermore, to detect the mouse VEGF transcripts expressed from the endogenous gene, including all isoforms, an additional set of specific primers and probe sequences for the 5′-UTR of the native mRNA were designed with Primer Express software 3.0 (Applied Biosystems): EndoV forward: 5′-GACGGGCCTCCGAAACC; EndoV reverse: 5′-TGGTGGAGGTACAGCAGTAAAGC; EndoV probe, 5′-FAM-AACTTTCTGCTCTCTTGGGTGCACTGGAC-TAMRA. The cycling parameters were: 50°C for 2 min, followed by 95°C for 10 min and 40 cycles of denaturation at 95°C for 15 seconds and annealing/extension at 60°C for 1 min. All primers were used at 400 n*M*, the ExoV probe at 400 n*M*, and the EndoV probe at 100 n*M*. Reactions were performed in triplicate for each template, averaged, and normalized to expression of the 18S housekeeping gene (Applied Biosystem assay, Hs99999901_s1).

qRT-PCR was also performed on genomic DNA to quantify the number of myoblasts engrafted after implantation by measuring the amount of stably integrated LacZ retroviral construct. A reference curve was constructed for each of the different myoblast clonal populations with a 10-fold dilution series between 1 and 10^6 cells, using which the ΔCt data of each sample could be transformed into the corresponding absolute cell numbers. LacZ primer and probe sequences and reaction concentrations were previously published (Banfi *et al.*, 2012).

In vitro *assay of endothelial cell activation*

Human umbilical vein endothelial cells (HUVEC) were used between passage 3 and 5 and cultured as described previously (Witzenbichler *et al.*, 1998). Mouse aortic endothelial cells (MAEC) were obtained from E. Battegay (University Hospital of Zurich, Switzerland) and cultured in high-glucose DMEM (Sigma-Aldrich) supplemented with 10% FBS (HyClone), 1 m*M* sodium pyruvate (Gibco, Invitrogen), 0.1 m*M* MEM Non-Essential Amino Acids (Gibco,

Invitrogen), 2 m*M* glutamine (Gibco, Invitrogen), 100 U/ml penicillin, and 100 μg/ml streptomycin (Gibco, Invitrogen).

HUVEC were seeded into gelatin-coated six-well cell culture plates at 4×10^5 cells/well and grown to confluency for 3 days without further medium changes. MAEC were seeded into six-well cell culture plates at 1.5×10^5 cells/well and grown to confluency. Subsequently, cells were serum starved and stimulated with 50 ng/ml of human VEGF-A_{165} or mouse VEGF-A_{164} (R&D System) for 6 hr. Total RNA was extracted using RNeasy kit (Qiagen) and reverse-transcribed into cDNA with the Omniscript Reverse Transcription kit (Qiagen) according to the manufacturer's instructions. Quantitative real-time PCR (qRT-PCR) was performed on an ABI 7300 Real-Time PCR system (Applied Biosystems). As internal standard, 18S gene expression levels were used for normalization (TaqMan Gene Expression Assay, Hs99999901_s1, Applied Biosystem). The change in expression of human and mouse vascular cellular adhesion molecule-1 (VCAM1) upon VEGF-A stimulation was measured using customized TaqMan Gene Expression Assay Hs01003372_m1 and Mm01320970_m1, respectively (Applied Biosystem).

Statistical analysis

Data are presented as means ± standard error of the mean. The significance of differences was evaluated using one-way ANOVA with the Bonferroni correction for multiple comparisons. $P<0.05$ was considered statistically significant.

Results

Generation of mouse and human VEGF-expressing myoblasts

Primary mouse myoblasts, which already expressed LacZ from a different retroviral construct (Rando and Blau, 1994), were transduced with retroviruses expressing either mouse $VEGF_{164}$ (mV) or human $VEGF_{165}$ (hV) genes, linked to a truncated version of mouse or human CD8, respectively, as a marker to determine transduction efficiency by FACS (Misteli *et al.*, 2010; Wolff *et al.*, 2012) (Fig. 1A). Negative control myoblasts expressed mCD8 or hCD8, but no VEGF. Transduction efficiency was greater than 95% in all cases (Fig. 1B). The average VEGF expression, measured by ELISA, was 78.2 ± 2.6 ng/10^6 cells/day and 82.4 ± 5.4 ng/10^6 cells/day for the mV and hV populations, respectively.

In vivo *angiogenesis by heterogeneous mouse or human VEGF levels*

The primary transduced hV and mV populations were composed of cells expressing heterogeneous VEGF levels, depending on the number and genomic location of integrated vector copies. As shown in Figure 1C, 4 weeks after implantation into auricular muscles of SCID mice (n = 8 per cell type), neither mCD8 nor hCD8 control cells affected the capillary networks around transduced fibers. On the other hand, mV myoblasts caused the growth of large numbers of aberrant, bulbous vascular structures, which correlated with very limited stable engraftment of VEGF-expressing cells by X-gal staining, as previously described (Ozawa *et al.*, 2004). Surprisingly, expression of similarly high and heterogeneous levels of human $VEGF_{165}$ by hV myoblasts induced a robust increase in the density of homogeneous normal capillaries around transgenic fibers, but no instances of aberrant vascular structures could be detected in any of the implanted tissues.

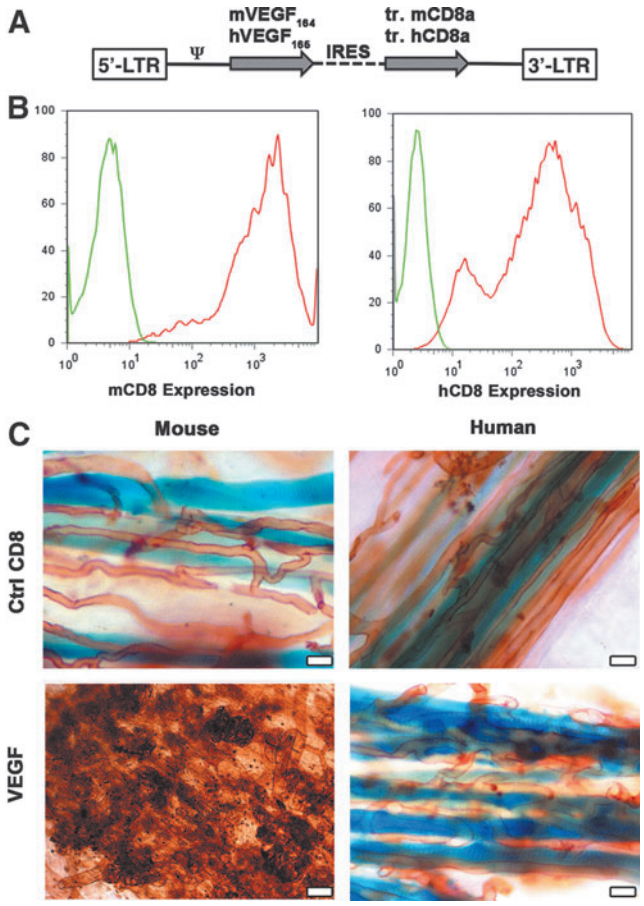

FIG. 1. Heterogeneous expression of human $VEGF_{165}$ induces only normal angiogenesis. **(A)** Maps of the bicistronic retroviral vectors carrying the coding sequence of murine VEGF ($mVEGF_{164}$) or human VEGF ($hVEGF_{165}$) and of a truncated version of murine or human CD8a (tr.CD8a), linked through an internal ribosome entry sequence (IRES). **(B)** Heterogeneous and high levels of expression of the VEGF-IRES-CD8 cassettes were detected by tracking mouse and human CD8a (mCD8 and hCD8, respectively) by flow cytometry in the primary populations of transduced myoblasts (red curves) and compared to nontransduced cells (negative control, green curves). **(C)** Whole-mount lectin staining (brown) of blood vessels 4 weeks after implantation of CD8 control cells (Ctrl CD8) and VEGF myoblasts expressing heterogeneous levels of either murine or human VEGF in the auricularis posterior muscle (n = 5–8 for all groups). Myoblasts engraftment was tracked by X-Gal staining (blue). Heterogeneous murine VEGF levels caused the widespread growth of aberrant angioma-like structures, whereas heterogeneous human VEGF levels induced only morphologically normal capillaries. Size bar = 50 μm in all panels. Color images available online at www.liebertpub.com/hgtb

Distribution of VEGF expression levels in the hV and mV populations

In order to determine why the heterogeneous hV population did not induce any aberrant angiogenesis, we asked whether the distribution of human VEGF expression levels by individual cells in the population might be different and

possibly skewed toward lower values than that of the mouse VEGF myoblasts. Therefore, single cells were isolated to obtain clonal populations, and their human VEGF production was measured and compared to that of mouse VEGF by similarly isolated mV clones, previously generated (Misteli *et al.*, 2010). Twenty-one hV clones were randomly isolated by single-cell FACS-sorting and found to secrete a wide range of $hVEGF_{165}$ levels (5.4 ± 0.9 to 254 ± 39 ng/10^6 cells/day). This range was similar to that of $mVEGF_{164}$ production by 15 mV clones (0.8 ± 0.1 to 142.55 ± 10 ng/10^6 cells/day). Analysis of the distribution of VEGF levels showed that both mV and hV populations secreted similarly spread levels over a wide range, without an enrichment for specific levels in either population (Fig. 2).

Microenvironmental dose-dependent angiogenesis by mouse and human VEGF

To rigorously compare the dose-dependent effects of human $VEGF_{165}$ to those previously described for mouse $VEGF_{164}$, hV and mV clones secreting matched VEGF levels were selected and injected into the ear and leg muscles of SCID mice. As shown in Figure 3A, clones were chosen that produced either a low or a high mouse $VEGF_{164}$ level, which were previously shown to induce normal and aberrant angiogenesis in mouse muscle, respectively (Ozawa *et al.*, 2004) ($mV_{low} = 40.5 \pm 4$ ng/10^6 cells/day and $mV_{high} = 133.6 \pm 13.4$ ng/10^6 cells/day). Matching hV clones produced similar and also higher levels of human $VEGF_{165}$ ($hV_{low} = 32.2 \pm 2.8$ ng/10^6 cells/day, $hV_{high1} = 129.9 \pm 7.5$ ng/10^6 cells/day and $hV_{high2} = 253.7 \pm 44.8$ ng/10^6 cells/day). The stability of VEGF secretion by the integrated retroviral constructs was periodically assessed by ELISA during expansion *in vitro* of all selected clones over at least 10 passages, corresponding to about 30 population doublings. In agreement with our previous results (Ozawa *et al.*, 2004; Misteli *et al.*, 2010), VEGF production was within 10% of reference levels during expansion, confirming that the clones reproducibly secreted predictable amounts of VEGF.

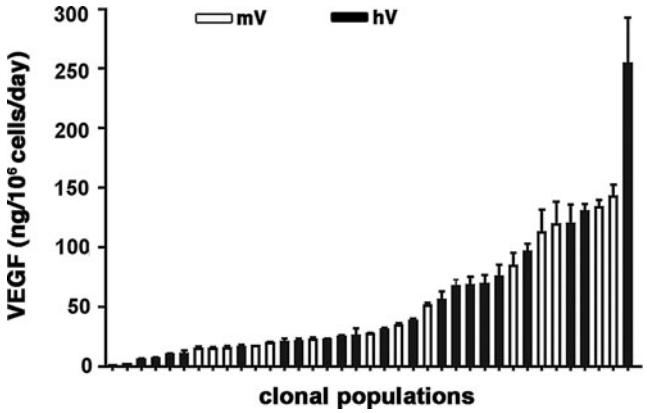

FIG. 2. Distribution of VEGF levels in clonal populations of myoblasts expressing murine or human VEGF. Single myoblast clones expressing either mouse or human VEGF were isolated from the polyclonal populations and their VEGF expression *in vitro* was quantified by enzyme-linked immunosorbent assay (ELISA), showing that both populations had a similar distribution of VEGF expression levels in individual cells. White bars = murine VEGF (mV)-expressing myoblasts; black bars = human VEGF (hV)-expressing myoblasts.

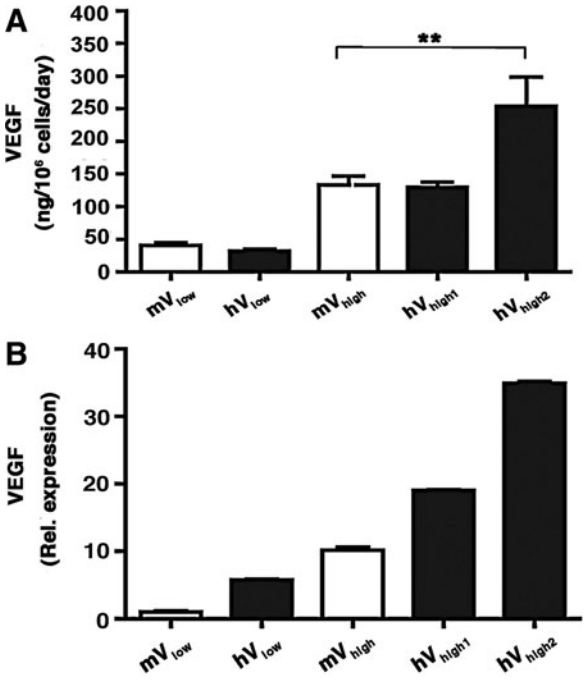

FIG. 3. Human and murine VEGF production by selected clones. Five clones were selected: two clones expressing either mouse (mV_{low}) or human (hV_{low}) VEGF at low levels and three clones expressing either mouse (mV_{high}) or human (hV_{high1}, hV_{high2}) VEGF at high levels. *In vitro* VEGF expression was measured by ELISA **(A)** and further confirmed by quantitative reverse-transcriptase polymerase chain reaction (qRT-PCR) **(B)**. $^{**}p < 0.01$.

The quantification of the amount of secreted human and murine VEGF protein by ELISA requires the use of distinct species-specific antibody pairs, which may affect the precise comparison of VEGF production between the two families of clones. Therefore, the relative expression levels of all selected clones were independently quantified by qRT-PCR ($n = 4$ per clone). A specific primer set was designed to recognize a viral construct-specific sequence, which is identical in the human and mouse expression cassettes, ensuring that results were comparable between all transduced populations. These results confirmed that in all cases the hV clones expressed similar or higher VEGF levels than the corresponding mV clones (Fig. 3B).

As shown in Figure 4A, 4 weeks after implantation in ear muscles, low levels of both human and mouse VEGF induced robust angiogenesis, comprising only homogeneous, normal capillaries. High mouse $VEGF_{164}$ expression gave rise to abundant aberrant vascular structures, as expected. However, a similarly high level of $hVEGF_{165}$ (clone hV_{high1}) induced only normal angiogenesis. Remarkably, even the hV_{high2} clone, which secreted double the amount of human $VEGF_{165}$, did not induce any angioma-like structures, but only normal and homogeneous capillary networks (Fig. 4A). In the presence of high mouse $VEGF_{164}$ expression, X-gal staining again showed very limited stable engraftment of VEGF-expressing myoblasts, contrary to the conditions inducing normal angiogenesis. Interestingly, and in agreement with our previously reported data (Ozawa *et al.*, 2004; von Degenfeld *et al.*, 2006; Misteli *et al.*, 2010), aberrant vascular structures continued growing into macroscopic angiomas

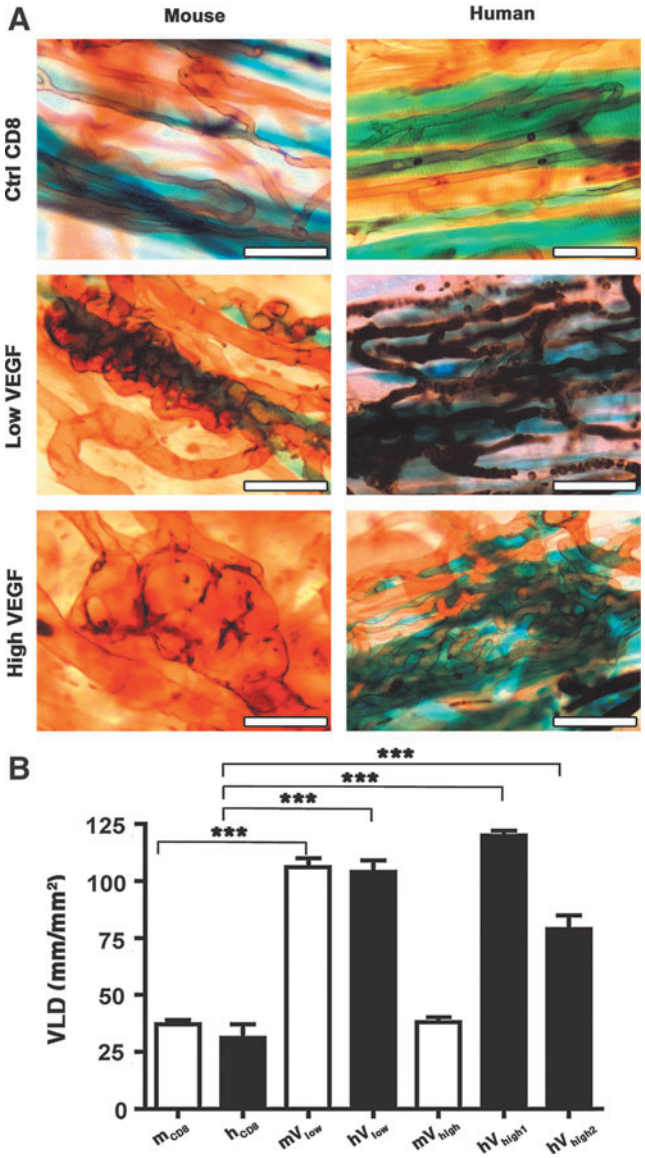

FIG. 4. Human $VEGF_{165}$ induces only normal angiogenesis despite high levels of expression. **(A)** Whole-mount lectin staining (brown) of vascular networks induced by control cells (Ctrl CD8) and mV and hV clonal populations. Myoblast engraftment was tracked by X-Gal staining (blue). Four weeks after myoblast implantation, low murine and human VEGF levels induced only morphologically normal capillaries. High murine VEGF levels gave rise to aberrant angioma-like vascular structures, whereas even higher levels of human VEGF (clone hV_{high2}) induced only normal angiogenesis (n = 5–8 for all groups). Vessels in the human low VEGF panel appear darker because they still contain some red blood cells. Size bar = 50 μm in all panels. **(B)** Quantification of the vessel length density (VLD) in vascular networks induced by the selected clones. ***$p < 0.001$. Color images available online at www.liebertpub.com/hgtb

after delivery of a high mouse $VEGF_{164}$ level despite its limited duration of expression, and we have previously found that this growth still depends on VEGF signaling, likely of endogenous origin (Ozawa *et al.*, 2004).

The amount of angiogenesis induced in the different conditions was quantified by measuring the vessel length density (VLD) in the cell implantation areas (n = 4 – 7/group). As shown in Figure 4B, low levels of both mouse and human VEGF caused a similarly large increase in VLD compared to control cells (106 ± 4 and $104 \pm 5\,mm/mm^2$, respectively, compared to 38 ± 2 and $31 \pm 6\,mm/mm^2$ with mCD8 and hCD8 cells; $p < 0.001$). VLD in areas implanted with the mV_{high} clone was not significantly increased compared to control areas ($38 \pm 2\,mm/mm^2$), as normal networks were replaced by large aberrant vascular structures, which show heterogeneously dilated diameters, but do not contribute an appreciable increase in vessel length. However, the normal capillaries induced by both clones expressing high levels of human $VEGF_{165}$ significantly increased VLD compared to control cells ($79 \pm 6\,mm/mm^2$ and $120 \pm 2\,mm/mm^2$ respectively; $p < 0.001$) to an extent similar to that induced by low VEGF levels.

Vascular maturation

We further analyzed the morphology and maturation of vascular networks induced by specific levels of human and mouse VEGF in the tibialis anterior (leg) muscles of SCID mice. Four weeks after injection (n = 4/group), implanted myoblasts, which expressed LacZ, were visualized by X-gal staining (Fig. 5A). Similarly to the implantations in ear muscles, stably engrafted transgenic fibers were found along needle tracks with similar frequency in all muscles, except in the presence of the angioma-like structures induced by high levels of murine VEGF (white asterisks in Fig. 5A), where only rare LacZ-positive single cells could be detected in the areas of injection. As shown in Figure 5B, low levels of both mouse and human VEGF caused an increased density of normal pericyte-covered capillaries around the transduced myofibers, compared to muscles implanted with control cells, while high levels of mouse VEGF induced aberrant angioma-like structures, devoid of pericytes and covered with a thick smooth muscle layer. However, in agreement with the results obtained in the ear muscles, expression of similar or even higher levels of human $VEGF_{165}$ only induced normal pericyte-covered capillary networks and no aberrant vascular structures (hV_{high2} clone shown in Fig. 5B).

In vivo *kinetics of VEGF expression*

Lastly, we sought to verify the possibility that the expression of human VEGF by the hV_{high} clones could decrease more rapidly than that of mouse VEGF by the mV_{high} clone after implantation *in vivo*, leading to a lower effective VEGF production in the tissue. Therefore, VEGF protein and mRNA levels were determined immediately after injection of mV_{high}, hV_{high1}, and hV_{high2} clones in tibialis anterior muscles, as well as at 7 and 14 days later (n = 4 per each group and time-point). Exogenous VEGF expression was quantified by qRT-PCR using the same primer set described above, which recognizes a sequence specific for the viral expression cassette and normalized by the relative myoblast engraftment in each sample, so as to account for the variability in cell death following injection. Myoblast engraftment in each sample was quantified by measuring the amount of stably integrated LacZ retroviral genomes by qRT-PCR and comparing this to a specific reference curve for each population. As expected, total VEGF protein dropped significantly in all cases during the first 7 days after implantation (Fig. 6A), as

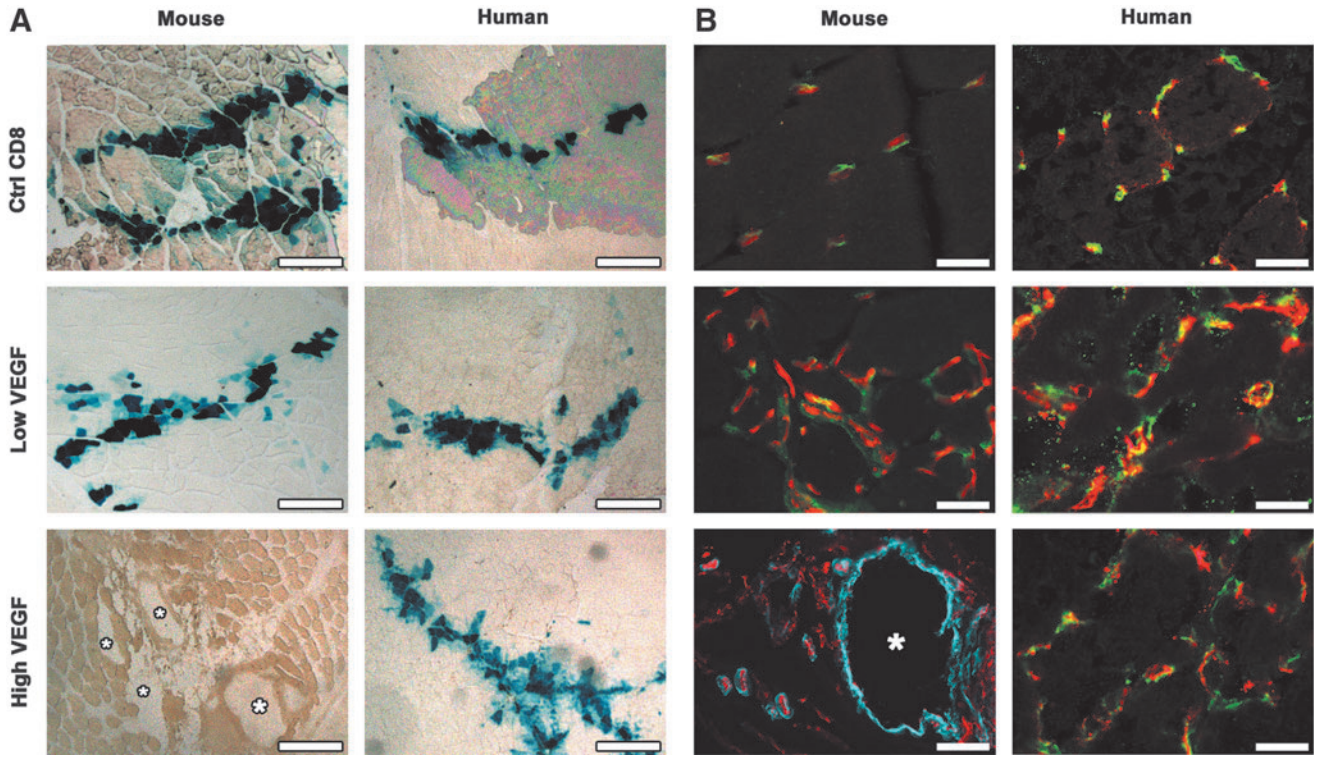

FIG. 5. High levels of human $VEGF_{165}$ induce mature capillaries rather than angiomas. **(A)** Myoblast engraftment was tracked by X-gal staining (blue) 4 weeks after implantation of control cells (Ctrl CD8) or mV and hV clones expressing low and high VEGF levels. In the presence of angiomas (white asterisks) induced by high levels of mouse VEGF very few myoblasts survived after 4 weeks, whereas in all other conditions consistent and stable engraftment was observed around the implantation needle tracks. **(B)** Vascular structures induced in the areas of engraftment 4 weeks after implantation were immunostained with antibodies against CD31 (endothelium, in red), NG2 (pericytes, in green), and SMA (smooth muscle cells, in cyan) in frozen sections of implanted limb muscles. Low levels of both mouse and human VEGF induced normal pericyte-covered capillaries and the aberrant angioma-like vascular structures caused by high mouse VEGF levels (white asterisk) were covered by a thick layer of SMA^+ cells but no pericytes. However, even higher levels of human VEGF (clone hV_{high2}) gave rise only to mature capillaries, covered with normal pericytes positive for NG2 and negative for SMA. Size bar = 500 μm in **(A)** and 50 μm in **(B)**. Color images available online at www.liebertpub.com/hgtb

about 90% of the myoblasts do not engraft and the retroviral promoter is down-regulated. However, despite a certain variability, both protein and mRNA measurements confirmed that *in vivo* expression of human $VEGF_{165}$ was similar or higher than that of mouse $VEGF_{164}$ at all time-points (Fig. 6A and B). The expression of endogenous VEGF was determined by qRT-PCR using specific primers spanning the 5′-UTR sequence, which is absent in the retroviral cassette, and the results did not show any significant changes between groups at all time-points (data not shown).

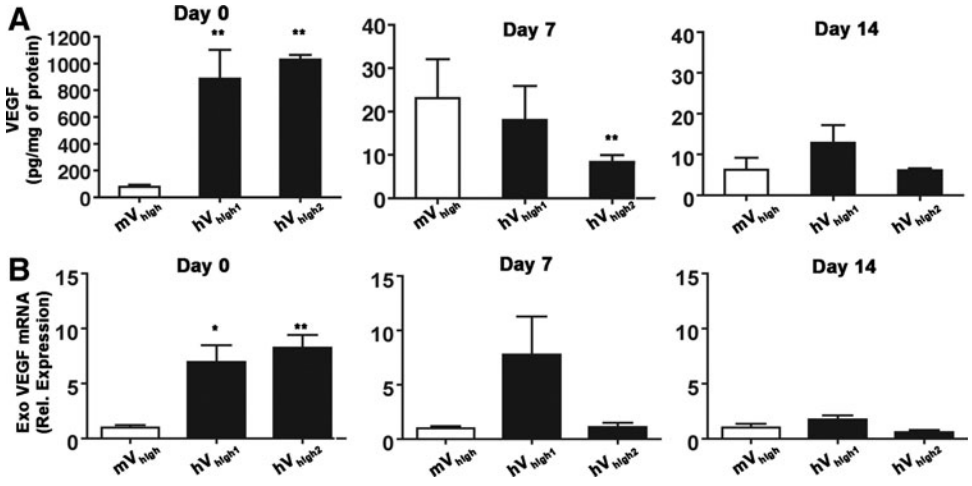

FIG. 6. *In vivo* expression of human $VEGF_{165}$ persists at similar or higher levels than that of mouse VEGF over 2 weeks. *In vivo* expression by mV and hV clones was quantified immediately after cell injection (Day 0), after 1 (Day 7), or 2 weeks (Day 14), both by ELISA **(A)** and qRT-PCR **(B)** on whole-muscle extracts, confirming that expression of hV clones was similar or higher than the corresponding mV clone up to 2 weeks after implantation. Exo. VEGF, exogenous vector-derived VEGF; *$p < 0.05$ and **$p < 0.01$ vs mV_{high}.

Efficacy of VEGF receptor signaling activation by mouse and human VEGF

Finally, in order to determine the mechanism by which human and mouse VEGF caused different effects at similarly high doses, we asked whether the two factors had an intrinsically different efficiency in signaling through their cognate receptors in mouse and human endothelial cells, respectively. Therefore, MAEC and HUVEC were stimulated with 50 ng/ml of either mouse $VEGF_{164}$ or human $VEFG_{165}$, and the relative signaling activation was assessed by measuring the induced expression of its direct target gene vascular cell adhesion molecule-1 (VCAM-1) (Schweighofer *et al.*, 2009). As shown in Figure 7, both factors were similarly efficient in driving VCAM-1 expression in syngenic endothelial cells (25.5-fold for mouse VEGF and 20.7-fold for human VEGF, compared to the unstimulated condition). However, mouse VEGF was significantly more efficient than human VEGF on mouse endothelial cells, and conversely human VEGF was more efficient on human endothelial cells, suggesting that human VEGF may display different dose-dependent effects in a mouse model due to a lower efficacy in activating signal transduction in mouse endothelial cells compared to the syngenic mouse VEGF.

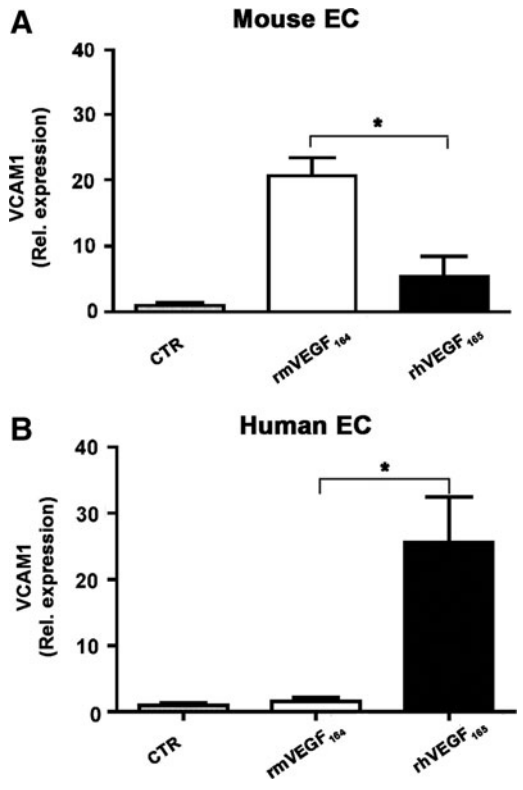

FIG. 7. The efficacy of VEGF-R signalling by mouse and human VEGF is species-specific. The induction of expression of the VEGF-A target gene VCAM1 was measured by qRT-PCR in human and murine endothelial cells (EC) after stimulation with 50 ng/ml of either recombinant murine or human VEGF ($rmVEGF_{164}$ and $rhVEGF_{165}$, respectively). Results are shown as relative expression compared to the control condition without VEGF stimulation (CTR). *$p < 0.05$.

Discussion

By taking advantage of a highly controlled cell-based platform for expression of specific VEGF levels in skeletal muscle, we could rigorously compare the dose-dependent effects of human and mouse $VEGF_{165/164}$ in a widely employed murine preclinical model. Although human $VEGF_{165}$ was similarly effective to mouse $VEGF_{164}$ in inducing normal angiogenesis at low doses, it differed dramatically from the syngenic factor in the potential to cause the growth of aberrant angioma-like vascular structures at higher doses. In fact, while clones expressing more than about 100 ng/10^6 cells/day of $mVEGF_{164}$ invariably caused the appearance of angiomas by 4 weeks, even 250 ng/10^6 cells/day of $hVEGF_{165}$ induced only the growth of physiological capillary networks. However, our results shown in Figure 7 suggest that this is unlikely to reflect a fundamental biological difference between the human and murine factors, but rather a lower potency of human $VEGF_{165}$ in stimulating the mouse VEGF receptors and vice versa.

There are no studies directly comparing the effects of human and syngenic VEGF in preclinical animal models. Angioma formation has been reported extensively after $mVEGF_{164}$ expression in different murine tissues, such as skeletal and cardiac muscle with skin and fat (Springer *et al.*, 1998; Lee *et al.*, 2000; Pettersson *et al.*, 2000; Ozawa *et al.*, 2004), in agreement with our results. On the other hand, the induction of angiomas by over-expression of $hVEGF_{165}$ has been described only rarely. There are no reports of $hVEGF_{165}$-induced angiomas in mouse tissues, while one study (Schwarz *et al.*, 2000) described the appearance of angiomas in the heart of rats after injection of a high dose of a $hVEGF_{165}$ plasmid (500 μg DNA) in a single intramyocardial injection, probably leading to a localized hotspot of very strong expression. Rabbit $VEGF_{165}$ shares a greater degree of homology with the human sequence (14 amino acid [aa] difference) compared with mouse $VEGF_{164}$ (19 aa difference). In the skeletal muscle of rabbits, delivery of a single high dose of $hVEGF_{165}$-expressing adeno-associated viral (AAV) vectors (10^{11} particles) caused aberrant vascular growth, the formation of functional arterio-venous shunts and muscle fibrosis, but only after at least 6 months of sustained expression (Zacchigna *et al.*, 2007; Karvinen *et al.*, 2011). One dose-escalation study investigated the effects of delivering from 10^9 to 10^{11} viral particles of $hVEGF_{165}$-expressing adenovirus (AV) to rabbit skeletal muscle and found dose-dependent differences both in vessel morphology and functional improvement (Korpisalo *et al.*, 2011). However, the short duration of expression afforded by the immune clearance of AV vectors prevented the evaluation of angioma formation. In human clinical trials, where low vector doses are dictated by safety concerns, only one study reported the transient appearance of spider angiomas at a site downstream of the treated tissue after delivery of $hVEGF_{165}$ plasmid (Isner *et al.*, 1996).

But why did human VEGF show reduced efficacy selectively in inducing aberrant angiogenesis and not also normal vascular growth? In fact, low doses of both factors effectively increased vessel length density by the same amount (Fig. 4B). We recently found that therapeutic over-expression of VEGF in skeletal muscle does not cause vascular growth by sprouting, but rather through an initial vascular enlargement

followed by intussusceptive remodeling and longitudinal splitting (Gianni-Barrera *et al.*, 2013). We also found that both normal and aberrant angiogenesis are induced through the same process in these conditions. However, high doses of $mVEGF_{164}$ cause a significantly greater initial enlargement than lower doses and, while intussusception is initiated in both cases, pillars fail to complete in the vessels of larger diameter, leading to a failure to split into normal capillaries and to the continued circumferential growth of affected vascular segments into angioma-like structures. Therefore, it is possible to envision that a reduced efficacy of $hVEGF_{165}$ in activating mouse VEGF receptor signaling may lead to lesser vascular enlargement and allow successful completion of intussusceptive remodeling despite higher VEGF doses, thereby avoiding the growth of aberrant angioma-like structures. On the other hand, at lower doses, which allow vascular splitting to complete successfully in either case, the different potency of the two factors would not produce evident consequences on either the morphology or amount of induced vessels.

It is clear that $hVEGF_{165}$ is capable of inducing angioma growth also in animal models if expressed at a sufficiently high level and a prolonged time. Therefore, our findings can in no way be taken as evidence that a tight control of VEGF levels would not be required in a clinical application of $hVEGF_{165}$. Rather, they have implications for the preclinical evaluation of VEGF-based strategies to treat ischemic conditions. In fact, it has been recognized that the complexity of growth factor dosing may be pivotal for the lack of efficacy in VEGF gene therapy clinical trials (Yla-Herttuala *et al.*, 2004), and it has been advocated that preclinical development of vectors should include the routine analysis of "STED" parameters: (1) Spread through the tissue; (2) transfection efficiency; (3) expression strength; and (4) duration of expression (Yla-Herttuala, 2006). Within this framework, our data suggest that, in a preclinical animal model, parameter "E" will depend not only on the amount of factor produced but also on the species-dependent potency of the human protein in that animal model. Therefore, the results of preclinical dose-escalation studies of the human factor in animal models should be interpreted with caution, as species-specific differences may specifically mask important dose-dependent side effects.

In conclusion, our data suggest that only dose-finding Phase-I clinical studies can accurately determine the safety profile of VEGF gene therapy approaches. In this respect, it would be advantageous to employ a tool that allows the controlled delivery of increasing doses, while also ensuring a homogeneous distribution of expression levels *in vivo*, in order to avoid hotspots and exploit the therapeutic window of VEGF (Banfi *et al.*, 2005). We recently developed such a tool for cell-based VEGF gene delivery, whereby high-throughput FACS purification of transduced progenitors allows the rapid generation of populations homogeneously expressing a pre-defined VEGF level (Misteli *et al.*, 2010; Wolff *et al.*, 2012).

Acknowledgments

The cDNA encoding $hVEGF_{165}$ was a kind gift from Peter Boekstegers (Klinikum Grosshadern, Munich, Germany). This work was supported by an Intramural Research Grant of the Department of Surgery (Basel University Hospital), by the European Union FP7 grants MAGISTER (CP-IP 214685) and ANGIOSCAFF (CP-IP 214402), by the Swiss National Science Foundation grant 127426, and by a Swiss Heart Foundation grant to A.B.

Author Disclosure Statement

No competing financial interests exist.

References

Banfi, A., Springer, M.L., and Blau, H.M. (2002). Myoblast-mediated gene transfer for therapeutic angiogenesis. Methods Enzymol. 346, 145–57.

Banfi, A., Von Degenfeld, G., and Blau, H.M. (2005). Critical role of microenvironmental factors in angiogenesis. Curr. Atheroscler. Rep. 7, 227–34.

Banfi, A., Von Degenfeld, G., Gianni-Barrera, R., *et al.* (2012). Therapeutic angiogenesis due to balanced single-vector delivery of VEGF and PDGF-BB. FASEB J 26, 2486–97.

Carmeliet, P. (2000). VEGF gene therapy: stimulating angiogenesis or angioma-genesis? Nat. Med. 6, 1102–3.

Carmeliet, P. (2003). Angiogenesis in health and disease. Nat. Med. 9, 653–60.

Gianni-Barrera, R., Trani, M., Fontanellaz, C., *et al.* (2013). VEGF over-expression in skeletal muscle induces angiogenesis by intussusception rather than sprouting. Angiogenesis 16, 123–36.

Gupta, R., Tongers, J., and Losordo, D.W. (2009). Human studies of angiogenic gene therapy. Circ. Res. 105, 724–36.

Isner, J.M., Pieczek, A., Schainfeld, R., *et al.* (1996). Clinical evidence of angiogenesis after arterial gene transfer of phVEGF165 in patient with ischaemic limb. Lancet 348, 370–4.

Karvinen, H., and Yla-Herttuala, S. (2010). New aspects in vascular gene therapy. Curr. Opin. Pharmacol. 10, 208–11.

Karvinen, H., Pasanen, E., Rissanen, T.T., *et al.* (2011). Long-term VEGF-A expression promotes aberrant angiogenesis and fibrosis in skeletal muscle. Gene Ther. 18, 1166–72.

Korpisalo, P., Hytonen, J.P., Laitinen, J.T., *et al.* (2011). Capillary enlargement, not sprouting angiogenesis, determines beneficial therapeutic effects and side effects of angiogenic gene therapy. Eur. Heart J. 32, 1664–72.

Lee, R.J., Springer, M.L., Blanco-Bose, W.E., *et al.* (2000). VEGF gene delivery to myocardium: deleterious effects of unregulated expression. Circulation 102, 898–901.

Misteli, H., Wolff, T., Fuglistaler, P., *et al.* (2010). High-throughput flow cytometry purification of transduced progenitors expressing defined levels of vascular endothelial growth factor induces controlled angiogenesis in vivo. Stem Cells 28, 611–9.

Norgren, L., Hiatt, W.R., Dormandy, J.A., *et al.* (2007). Inter-society consensus for the management of peripheral arterial disease (TASC II). J. Vasc. Surg. 45 Suppl S, S5–67.

Ozawa, C.R., Banfi, A., Glazer, N.L., *et al.* (2004). Microenvironmental VEGF concentration, not total dose, determines a threshold between normal and aberrant angiogenesis. J. Clin. Invest. 113, 516–27.

Park, J.E., Keller, G.A., and Ferrara, N. (1993). The vascular endothelial growth factor (VEGF) isoforms: differential deposition into the subepithelial extracellular matrix and bioactivity of extracellular matrix-bound VEGF. Mol. Biol. Cell. 4, 1317–26.

Pettersson, A., Nagy, J.A., Brown, L.F., *et al.* (2000). Heterogeneity of the angiogenic response induced in different normal adult tissues by vascular permeability factor/vascular endothelial growth factor. Lab. Invest. 80, 99–115.

Rando, T.A., and Blau, H.M. (1994). Primary mouse myoblast purification, characterization, and transplantation for cell-mediated gene therapy. J. Cell Biol. 125, 1275–87.

Ruhrberg, C., Gerhardt, H., Golding, M., *et al.* (2002). Spatially restricted patterning cues provided by heparin-binding VEGF-A control blood vessel branching morphogenesis. Genes Dev. 16, 2684–98.

Schwarz, E.R., Speakman, M.T., Patterson, M., *et al.* (2000). Evaluation of the effects of intramyocardial injection of DNA expressing vascular endothelial growth factor (VEGF) in a myocardial infarction model in the rat—angiogenesis and angioma formation. J. Am. Coll. Cardiol. 35, 1323–30.

Schweighofer, B., Testori, J., Sturtzel, C., *et al.* (2009). The VEGF-induced transcriptional response comprises gene clusters at the crossroad of angiogenesis and inflammation. Thromb. Haemost. 102, 544–54.

Springer, M.L., and Blau, H.M. (1997). High-efficiency retroviral infection of primary myoblasts. Somat. Cell Mol. Genet. 23, 203–9.

Springer, M.L., Chen, A.S., Kraft, P.E., *et al.* (1998). VEGF gene delivery to muscle: potential role for vasculogenesis in adults. Mol. Cell. 2, 549–58.

Springer, M.L., Ozawa, C.R., Banfi, A., *et al.* (2003). Localized arteriole formation directly adjacent to the site of VEGF-induced angiogenesis in muscle. Mol. Ther. 7, 441–9.

Tagawa, M., Nakauchi, H., Herzenberg, L.A., and Nolan, G.P. (1986). Formal proof that different-size Lyt-2 polypeptides arise from differential splicing and post-transcriptional regulation. Proc. Natl. Acad. Sci. USA 83, 3422–6.

Von Degenfeld, G., Banfi, A., Springer, M.L., *et al.* (2006). Microenvironmental VEGF distribution is critical for stable and functional vessel growth in ischemia. FASEB J 20, 2657–9.

Witzenbichler, B., Maisonpierre, P.C., Jones, P., *et al.* (1998). Chemotactic properties of angiopoietin-1 and −2, ligands for the endothelial-specific receptor tyrosine kinase Tie2. J. Biol. Chem. 273, 18514–21.

Wolff, T., Mujagic, E., Gianni-Barrera, R., *et al.* (2012). FACS-purified myoblasts producing controlled VEGF levels induce safe and stable angiogenesis in chronic hind limb ischemia. J. Cell. Mol. Med. 16, 107–17.

Yla-Herttuala, S. (2006). An update on angiogenic gene therapy: vascular endothelial growth factor and other directions. Curr. Opin. Mol. Ther. 8, 295–300.

Yla-Herttuala, S., Markkanen, J.E., and Rissanen, T.T. (2004). Gene therapy for ischemic cardiovascular diseases: some lessons learned from the first clinical trials. Trends Cardiovasc. Med. 14, 295–300.

Zacchigna, S., Tasciotti, E., Kusmic, C., *et al.* (2007). In vivo imaging shows abnormal function of vascular endothelial growth factor-induced vasculature. Hum. Gene Ther. 18, 515–24.

Address correspondence to:
Dr. Andrea Banfi
Cell and Gene Therapy
Basel University Hospital
Hebelstrasse 20
Basel, CH-4031
Switzerland

E-mail: andrea.banfi@usb.ch

Dr. Thomas Wolff
Vascular Surgery
Basel University Hospital
Spitalstrasse 21
Basel, CH-4031
Switzerland

E-mail: thomas.wolff@usb.ch

Received for publication October 10, 2012;
accepted after revision January 20, 2013.

Published online: January 29, 2013.